Journal of Solid State Chemistry **153,** 174–179 (2000)
doi:10.1006/jssc.2000.8773, available online at http://www.idealibrary.com on IDEAL®

Highly Conductive Oxides, $CeVO_4$, $Ce_{1-x}M_xVO_{4-0.5x}$ (M = Ca, Sr, Pb) and $Ce_{1-y}Bi_yVO_4$, with Zircon-Type Structure Prepared by Solid-State Reaction in Air

Akiteru Watanabe

National Institute for Research in Inorganic Materials, 1-1 Namiki, Tsukuba, Ibaraki 305-0044 Japan
E-mail: watanakt@nirim.go.jp.

Received February 24, 2000; in revised form May 1, 2000; accepted May 11, 2000; published online June 29, 2000

The zircon-type phases, $CeVO_4$, $Ce_{1-x}M_xVO_{4-0.5x}$ ($0 \le x \le 0.41$ for M = Ca, $0 \le x \le 0.21$ for M = Sr, and $0 \le x \le 0.1$ for M = Pb) and $Ce_{1-y}Bi_yVO_4$ ($0 \le y \le 0.68$), have been prepared in air by heating the stoichiometric mixture of CeO_2, V_2O_5, $CaCO_3$, $SrCO_3$, PbO, and Bi_2O_3. During solid-state reaction, the spontaneous reduction of Ce(IV) to Ce(III) begins above 500°C and proceeds rapidly at about 666°C in conjunction with the melting of V_2O_5. All of these phases present high electrical conduction. In particular, the phases $Ce_{1-x}M_xVO_{4-0.5x}$ (M = Ca, Sr, and Pb) show excellently high values. The compound $CeVO_4$ is characterized as a p-type semiconductor by the Seebeck effect. © 2000 Academic Press

Key Words: **$CeVO_4$; $Ce_{1-x}M_xVO_{4-0.5x}$ (M = Ca, Sr, and Pb); $Ce_{1-y}Bi_yVO_4$; solid-state reaction; spontaneous reduction; high electrical conduction; p-type semiconductor; Seebeck effect.**

INTRODUCTION

A series of lanthanide vanadates, Ln(III)V(V)O_4 (Ln = lanthanide including Y), were extensively investigated by several researchers (1–18) from the crystal-chemical point of view. The structural studies under ambient conditions revealed that only $LaVO_4$ crystallizes with the monazite-type structure conforming to space group $P2_1/n$ (3, 5, 6, 11, 13, 15) and that the other $LnVO_4$'s have the zircon-type structure with $I4_1/amd$ (1–11, 13–18). The compounds were prepared by either wet chemical methods (3, 4, 15, 17) or the solid-state reaction between the starting oxides or salts (1, 2, 5–8, 10, 11, 13, 16, 18). Regarding $CeVO_4$, however, there seems to be confusion in the synthesis using solid-state technique. That is, $CeVO_4$ was obtained by the reaction between Ce(III) salts or its oxide and V_2O_5 under an inert atmosphere (16, 18) because of the instability of Ce(III) in air at high temperatures. On the other hand, many researchers (2, 5, 6, 10, 13) reported that $CeVO_4$ could be prepared by conventional solid-state reaction of CeO_2 and V_2O_5 in air. In particular, using TG–DTA method, Yoshimura and Sata (10) observed an *in situ* result of the formation of $CeVO_4$ by the reduction of Ce(IV) during the solid-state reaction of CeO_2 and V_2O_5 in air. Nevertheless, they did not check on this product further with respect to its properties.

The purpose of the present study is to reexamine the solid-state reaction between CeO_2 and V_2O_5 in air and to check electrical conductivity of $CeVO_4$. Furthermore, we have prepared highly electrically conductive solid solutions, (Ce, M)$VO_{4-\delta}$ where M = Ca, Sr, and Pb and (Ce, Bi)VO_4, which are isomorphous with $CeVO_4$.

EXPERIMENTAL PROCEDURES

The starting materials were 99.9% pure CeO_2 (Shin-Etsu Chemical Co., Ltd., Tokyo), V_2O_5 and PbO (Kojundo Chemical Laboratory Co., Ltd., Sakato), Bi_2O_3 (Iwaki Chemicals Ltd., Tokyo), and reagent-grade $CaCO_3$ and $SrCO_3$ (Nakarai Chemicals Ltd., Kyoto). To check the formation of $CeVO_4$ by solid-state reaction in air, the stoichiometric mixture ($CeO_2 : V_2O_5$ in a molar ratio of 2 : 1) was heated in a covered platinum crucible at 800°C for 50 h. In addition, syntheses of sample preparations of compositions $Ce_{1-x}M_xVO_{4-0.5x}$ ($0 < x \le 0.5$ for M = Ca, $0 < x \le 0.4$ for M = Sr, and $0 < x \le 0.2$ for M = Pb) and $Ce_{1-y}Bi_yVO_4$ ($0 < y \le 0.8$) were tried by solid-state reaction in air from the viewpoint of replacing part of Ce(III) in $CeVO_4$ by M(II) or Bi(III); the mixture of the desired proportions of the starting materials was heated at 850°C for 50 h or more. At the end of the reactions, the products were quenched by an air stream to room temperature. All products were examined by X-ray powder diffraction (XRPD) using Cu$K\alpha$ radiation and a diffracted-beam monochromator.

In order to confirm Ce(III) in $CeVO_4$ prepared above, a qualitative analysis was made with an oxidation method using persulfate (19) that is based on the fact that tetravalent cerium ion is yellow. At the same time, another qualitative

0022-4596/00 $35.00

analysis of Ce(IV) was also made using the *o*-phenanthroline ferrous sulfate indicator (20).

The oxygen contents of $CeVO_4$ and some solid solutions were checked by means of a Nitrogen/Oxygen Determinator (LECO TC-436AR). The sample weight was about 10 mg, and the oxygen content accuracy was $\pm 2\%$.

To examine the solid solubility extension by a parametric method (21), the precise lattice parameters were calculated by the least-squares method (22) on the observed XRPD data measured with a continuous scanning method at a scanning rate of 0.4° (2θ) min^{-1} over the angular range $15–135^\circ$ (2θ). The 2θ values were corrected using the external standard of a Si powder.

The thermally *in situ* observations of the solid state reaction of the above reactant systems were carried out using a simultaneous thermogravimetry–differential thermal analysis (TG–DTA) apparatus (Rigaku TG-8120). About 50 mg of the starting powder mixture put in a platinum sample holder underwent heating–cooling cycles in air to the maximum temperature of 950°C. The heating–cooling rates employed were 2, 3, 5, and 10°C min^{-1}. The reference material was α-Al_2O_3, and the temperature accuracy was ± 3°C.

The DC conductivity measurement was carried out on a sintered circular pellet (14 mm in diameter and about 2.5 mm thick) in the same way as described before (23). The platinum paste was used as electrodes.

RESULTS AND DISCUSSION

The product from the reaction $[2CeO_2 + V_2O_5]$ was blackish brown, and the XRPD pattern of it was undoubtedly connected to the typical zircon-type structure as shown in Fig. 1. The measured tetragonal lattice parameters were $a = 7.4016(1)$ Å and $c = 6.4980(1)$ Å. The existence of Ce(III) in this product was clearly recognized by the qualitative analysis; in contrast, Ce(IV) was not confirmed. In other words, polycrystalline $CeVO_4$ was readily prepared by solid-state reaction in air according to the following reaction formula as reported by Yoshimura and Sata (10):

$$2CeO_2 + V_2O_5 \rightarrow 2CeVO_4 + 0.5O_2. \quad [1]$$

The TG–DTA results of this reaction are shown in Fig. 2. Although the solid-state reaction starts at a temperature above 500°C depending on a heating rate, a sharp endothermic effect was always observed at about 666°C, at which the solid-state reaction proceeds rapidly and tends to the end of the reaction. This endothermic peak may be due to the

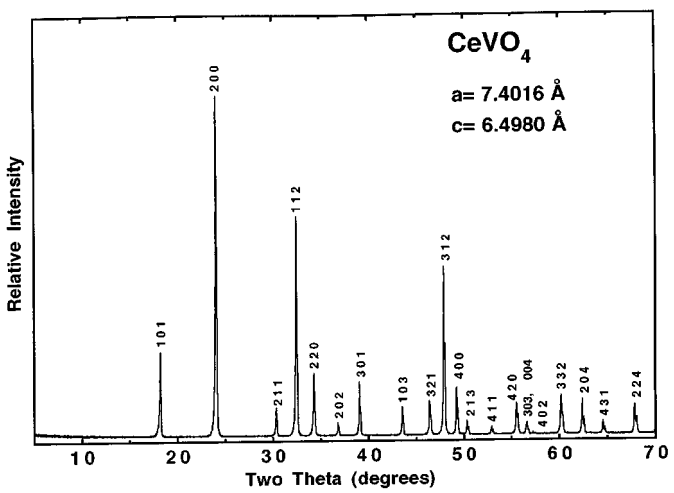

FIG. 1. XRPD pattern of $CeVO_4$ equilibrated at 800°C in air ($\lambda = \text{Cu}K\alpha$).

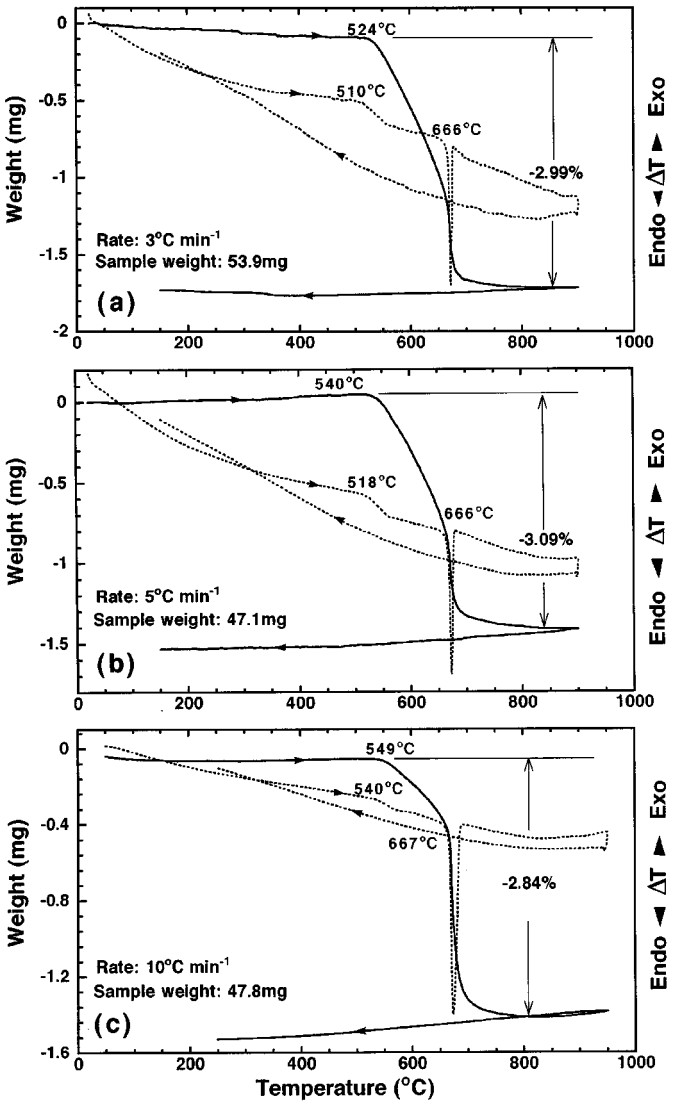

FIG. 2. TG–DTA curves of the reaction $[2CeO_2 + V_2O_5]$ for a heating and cooling cycle. The solid lines indicate TG, and the broken lines indicate DTA.

melting of V_2O_5 (mp = 690°C (24)). Furthermore, reaction formula [1] yields the calculated weight loss of 3.04% which agrees well with the observed results (Fig. 2a and 2b). The value of 2.84% in Fig. 2c is attributable to a relatively faster heating rate which brings about the incomplete solid-state reaction; in fact, after TG–DTA measurement, the XRPD showed that the sample contains a very small amount of CeO_2. Thus, we can conclude that the reaction formula [1] is completed quantitatively in air in its equilibrium state, such as the present conditions at 800°C for 50 h.

In the three-component systems $Ce_{1-x}M_xVO_{4-0.5x}$ (M = Ca, Sr, and Pb) and $Ce_{1-y}Bi_yVO_4$, since the XRPD of some products prepared at 850°C showed such a simple, clear pattern as Fig. 1, there exists a form of solid solution series with the zircon-type structure. Figures 3 and 4 show the variations of lattice parameters with composition. From these results, the solid solubility regions are determined as

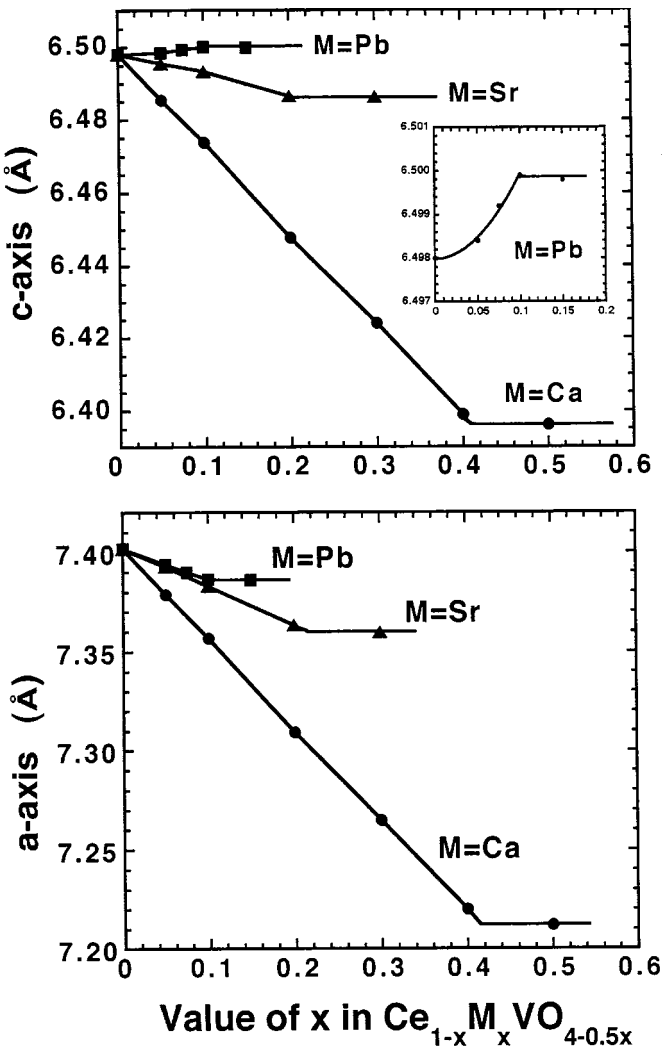

FIG. 3. Variation of lattice parameters (a and c) of $Ce_{1-x}M_xVO_{4-0.5x}$ (M = Ca, Sr, and Pb) with composition x.

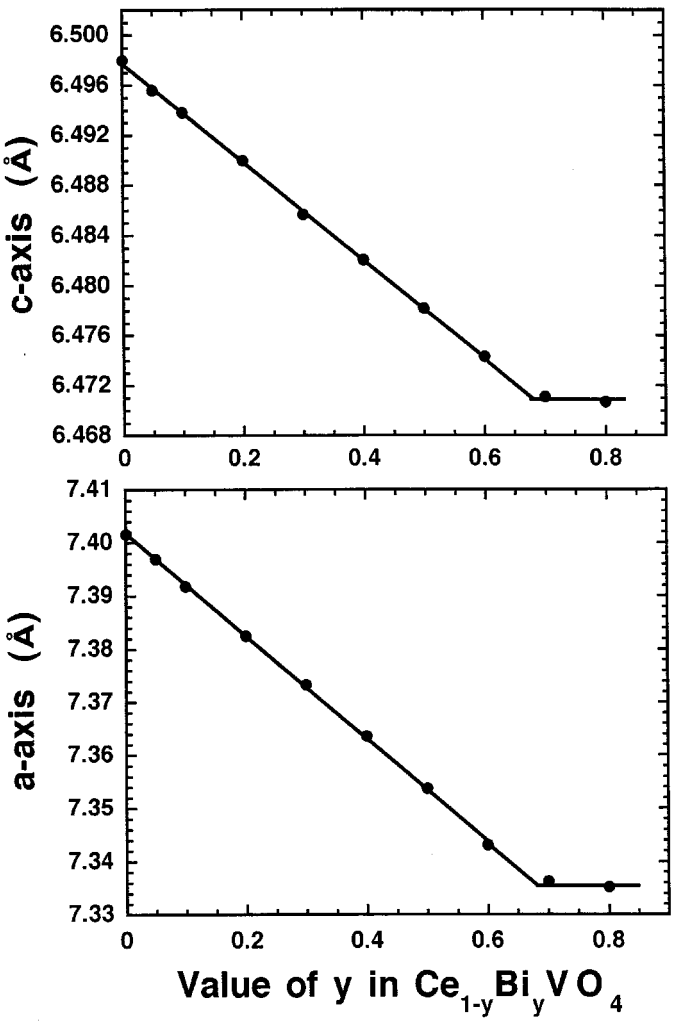

FIG. 4. Variation of lattice parameters (a and c) of $Ce_{1-y}Bi_yVO_4$ with composition y.

follows: $0 \le x \le 0.41$ for M = Ca, $0 \le x \le 0.21$ for M = Sr, and $0 \le x \le 0.1$ for M = Pb in $Ce_{1-x}M_xVO_{4-0.5x}$, and $0 \le y \le 0.68$ in $Ce_{1-y}Bi_yVO_4$ at 850°C. Except for M = Pb, all the results obey Vegard's rule well; both a and c axes decrease linearly with concentration of oxide additives. However, only the c axis length of $Ce_{1-x}Pb_xVO_{4-0.5x}$ varies abnormally and increases with x as shown in the inset of Fig. 3. Using ionic radii of M(II) in eight-coordination with which Ce(III) are present in the zircon-type structure, the above solid solubility regions are qualitatively explained. That is, the effective ionic radii (25) of Ce(III), Ca(II), Sr(II), and Pb(II) are respectively 1.14, 1.12, 1.26, and 1.29 Å. Since Ce(III) and Ca(II) have a similar size, the substitution of Ca(II) for Ce(III) yields the most extensive solubility region of three oxide additives. On the contrary, in the case of Pb(II), the relatively large size difference brings the narrowest solubility range and the deviation from the

Vegard's rule. In fact, we were unsuccessful in replacing Ce(III) by Ba(II) with an ionic radius of 1.42 Å. However, the extensive solid solubility range in $Ce_{1-y}Bi_yVO_4$ may be explained on the basis of the presence of the zircon-type $BiVO_4$ (26, 27) as well as an ionic radius of Bi(III), 1.17 Å; namely, although $BiVO_4$ crystallizes in the monoclinic form (28) by a conventional solid-state reaction, the zircon-type tetragonal form can be prepared by a precipitation method from an aqueous solution (26) or by aqueous processes (27). Therefore, the incorporation of Bi(III) into Ce(III)VO_4 leads to less distortion of the zircon-type lattice.

Figure 5 exhibits the TG–DTA results of the following solid-state reactions for the representative compositions within the solid solution of the above three-component systems:

$$1.8CeO_2 + 0.2CaCO_3 + V_2O_5 \rightarrow 2Ce_{0.9}Ca_{0.1}VO_{3.95} + 0.45O_2 + 0.2CO_2, \quad [2]$$

$$1.8CeO_2 + 0.2SrCO_3 + V_2O_5 \rightarrow 2Ce_{0.9}Sr_{0.1}VO_{3.95} + 0.45O_2 + 0.2CO_2, \quad [3]$$

$$1.9CeO_2 + 0.1PbO + V_2O_5 \rightarrow 2Ce_{0.95}Pb_{0.05}VO_{3.975} + 0.475O_2, \quad [4]$$

$$1.8CeO_2 + 0.1Bi_2O_3 + V_2O_5 \rightarrow 2Ce_{0.9}Bi_{0.1}VO_4 + 0.45O_2. \quad [5]$$

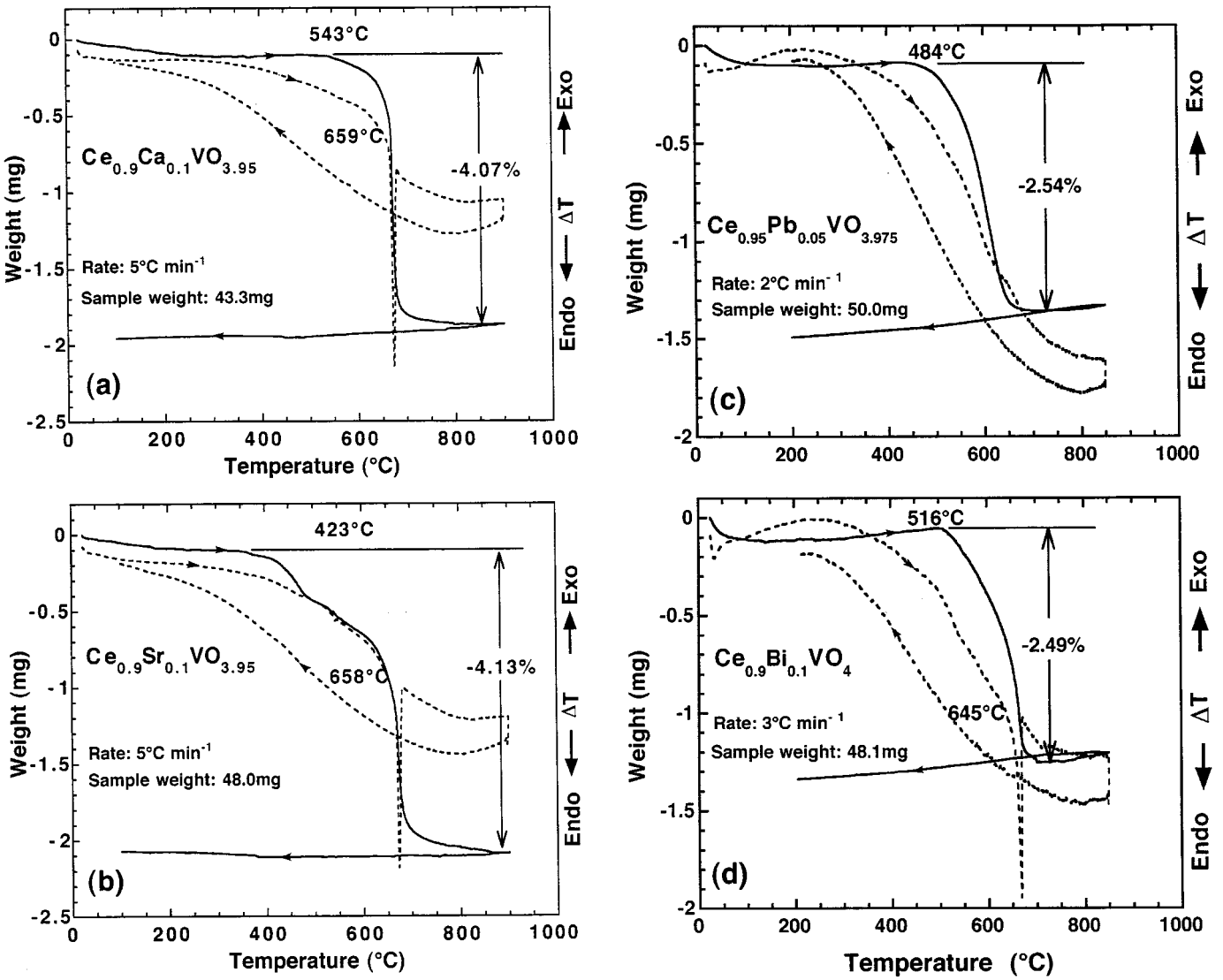

FIG. 5. TG–DTA curves of the following reactions: (a) $[1.8CeO_2 + 0.2CaCO_3 + V_2O_5]$, (b) $[1.8CeO_2 + 0.2SrCO_3 + V_2O_5]$, (c) $[1.9CeO_2 + 0.1PbO + V_2O_5]$, and (d) $[1.8CeO_2 + 0.1Bi_2O_3 + V_2O_5]$. The solid lines denote TG, and the broken lines denote DTA.

In reaction formulae from [2] to [5], the calculated weight loss is respectively 4.53%, 4.45%, 2.86%, and 2.67%. In contrast to the reaction formula [1], each measured weight loss shown in Fig. 5 is smaller than the calculated value. After TG–DTA measurement, a very small amount of CeO_2 in all the specimens was identified by the XRPD; at the same time, the reflections from the zircon-type structure were fairly broad. That is, the solid state reaction is more sluggish in the three-component systems than the two-component system under the present TG–DTA kinetic heating conditions. On the other hand, the pure zircon-type phase was easily obtained in the equilibrium state by isothermal heating at 850°C for 50 h or more as mentioned in the Experimental Procedures. Accordingly, the weight loss difference between the calculated and the measured is ascribed to the sluggishness of the solid state reactions of the above formulae.

The oxygen contents were measured on the following samples: $CeVO_4$, $Ce_{0.925}Pb_{0.075}VO_{3.9625}$, $Ce_{0.9}Ca_{0.1}VO_{3.95}$, $Ce_{0.9}Sr_{0.1}VO_{3.95}$, and $Ce_{0.9}Bi_{0.1}VO_4$. The results in wt% were 25.1 (calculated value, 25.1) for $CeVO_4$, 24.6 (24.4) for $M = Pb$, 26.0 (25.9) for $M = Ca$, 25.6 (25.4) for $M = Sr$, and 24.4 (24.4) for $Ce_{0.9}Bi_{0.1}VO_4$. The result of $Ce_{0.925}Pb_{0.075}VO_{3.9625}$ does not show the remarkable deviation from the calculated content in the same manner as those of $M = Ca$ and Sr; consequently, the oxidation state of the incorporated Pb may be kept in +II. Furthermore, since the measured values of all samples agree well with the calculated ones, and since no perceptible ignition loss except oxygen release was recognized as a result of solid state reaction at 850°C for 50 h or more, the compositional change may be negligibly small.

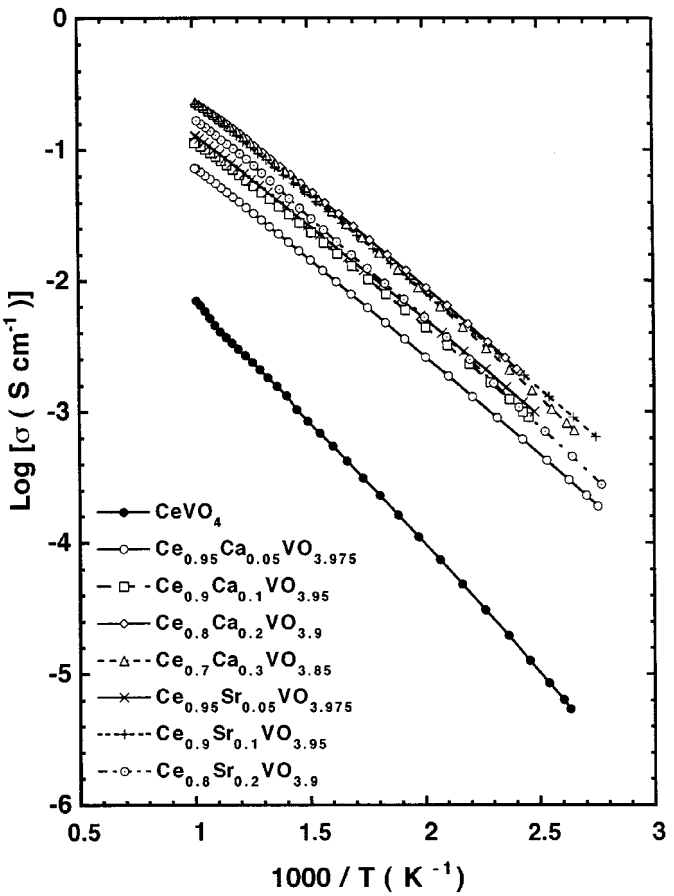

FIG. 6. Arrhenius plots of electrical conductivity σ of $CeVO_4$, $Ce_{1-x}M_xVO_{4-0.5x}$ (M = Ca and Sr) measured in air.

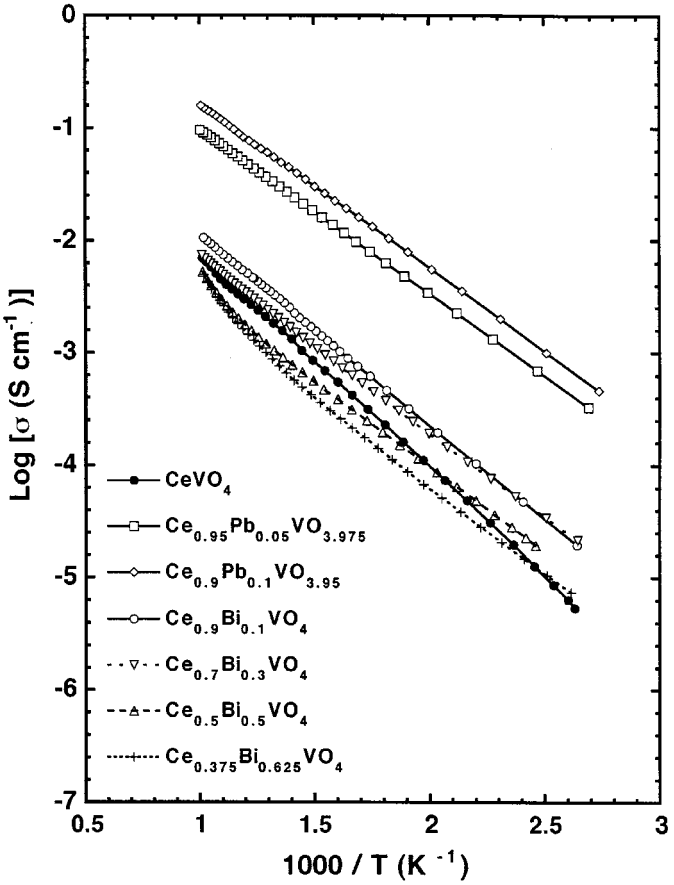

FIG. 7. Arrhenius plots of electrical conductivity σ of $CeVO_4$, $Ce_{1-x}Pb_xVO_{4-0.5x}$, and $Ce_{1-y}Bi_yVO_4$ measured in air.

Figures 6 and 7 represent the electrical conduction of $CeVO_4$ and some compositions in four kinds of solid solutions in the form of Arrhenius plots. While $CeVO_4$ shows relatively high conduction with the activation energy, $E_a \approx 0.37$ eV, the solid solutions $Ce_{1-x}M_xVO_{4-0.5x}$ (M = Ca, Sr, and Pb) give far higher conduction with $E_a \approx 0.30$ eV. On one hand, the conduction of $Ce_{1-y}Bi_yVO_4$ is slightly higher than that of $CeVO_4$ with $y < 0.5$ ($E_a \approx 0.31$ eV), and lower with $y \geq 0.5$ ($E_a \approx 0.30$ eV). It is noteworthy that incorporated divalent cations induce the higher electical conduction as well as the oxygen vacancies. Thus, we have checked the oxide-ion conduction by

measuring the electromotive force (EMF) using an oxygen concentration cell. As a result, not only $Ce_{1-x}M_xVO_{4-0.5x}$ but also $CeVO_4$ yielded no EMF up to 800°C. This result pointed out that the present oxides are n-type or p-type semiconductors. Therefore, we plan next to measure the Seebeck effect to decide which type of semiconductor is present. The result of $CeVO_4$ indicated a p-type one which present 0.5 mV K^{-1} at 200°C. Further analyses of the solid solutions are under way.

CONCLUSION

The zircon-type phases, $CeVO_4$, $Ce_{1-x}M_xVO_{4-0.5x}$ (M = Ca, Sr, and Pb), and $Ce_{1-y}Bi_yVO_4$, can be prepared in air by heating the stoichiometric mixture of CeO_2, V_2O_5, $CaCO_3$, $SrCO_3$, PbO, and Bi_2O_3. That is, the spontaneous reduction of Ce(IV) to Ce(III) occurs during solid-state reaction. All of these phases present high electrical conduction. In particular, the phases $Ce_{1-x}M_xVO_{4-0.5x}$ (M = Ca, Sr, and Pb) show excellently high values. The compound $CeVO_4$ is characterized as a p-type semiconductor by the Seebeck effect.

ACKNOWLEDGMENTS

This work was supported by CREST of Japan Science and Technology, and the author is indebted to Dr. Y. Aoki, Hokkaido University, for conducting the Seebeck effect measurements and to Mr. S. Takenouchi for chemical analyses.

REFERENCES

1. W. O. Milligan, L. M. Watt, and H. H. Rachford, Jr., *J. Phys. Colloid Chem.* **53,** 227 (1949).
2. W. O. Milligan and L. W. Vernon, *J. Phys. Chem.* **56,** 145 (1952).
3. M. K. Carron, M. E. Morse, and K. J. Murata, *Am. Mineral.* **43,** 985 (1958).
4. Powder Diffraction File, No. 12-757, International Center for Diffraction Data, Swarthmore, PA.
5. H. Schwarz, *Z. Anorg. Allg. Chem.* **323,** 44 (1963).
6. V. S. Stubican and R. Roy, *Z. Kristallogr.* **119,** 90 (1963).
7. J. R. Gambino and C. J. Guare, *Nature*, **198,** 1084 (1963).
8. E. Patscheke, H. Fuess, and G. Will, *Chem. Phys. Lett.* **2,** 47 (1968).
9. J. A. Baglio and G. Gashurov, *Acta Crystallogr. B* **24,** 292 (1968).
10. M. Yoshimura and T. Sata, *Bull. Chem. Soc. Jpn.* **42,** 3195 (1969).
11. E. J. Baran and P. J. Aymonino, *Z. Anorg. Allg. Chem.* **383,** 220 (1971).
12. J. A. Baglio and O. J. Sovers, *J. Solid State Chem.* **3,** 458 (1971).
13. H. Brusset, F. Madaule-Aubry, B. Blanck, J. P. Glaziou, and J. P. Laude,*Can. J. Chem.* **49,** 3700 (1971).
14. H. Fuess and A. Kallel, *J. Solid State Chem.* **5,** 11 (1972).
15. R. C. Ropp and B. Carroll, *J. Inorg. Nucl. Chem.* **35,** 1153 (1973).
16. K. J. Range, H. Meister, and U. Klement, *Z. Naturforsch. B* **45,** 598 (1990).
17. B. C. Chakoumakos, M. M. Abraham, and L. A. Boatner, *J. Solid State Chem.* **109,** 197 (1994).
18. L. H. Brixner and E. Abramson, *J. Electrochem. Soc.* **112,** 70 (1965).
19. F. D. Snell and C. T. Snell, *in* "Colorimetric Methods of Analysis," 3rd ed., Vol. II, Chap. 43. D. Van Nostrand Company, Toronto, Canada, 1967.
20. G. Charlot, *in* "L'Analyse Qualitative et les Réactions en Solution," 4th ed., Part II, Chap. 3. Masson et Cie, Paris, 1957.
21. B. D. Cullity, *in* "Elements of X-Ray Diffraction," 3rd printing, Chap. 12. Addison-Wesley, Reading, MA, 1967.
22. D. E. Appleman and H. T. Evans, Jr., *National Technical Information Service*, **PB-216**, 188 (1973).
23. A. Watanabe and T. Kikuchi, *Solid State Ionics* **21,** 287 (1986).
24. R.C. Weast (Ed.), *in* "CRC Handbook of Chemistry and Physics, 1st Student Edition," p. B-76. CRC Press, Boca Raton, FL, 1988.
25. R. D. Shannon, *Acta Crystallogr. A* **32,** 751 (1976).
26. A. K. Bhattacharya, K. K. Mallick, and A. Hartridge, *Mater. Lett.* **30,** 7 (1997).
27. A. Kudo, K. Omori, and H. Kato, *J. Am. Chem. Soc.* **121,** 11459 (1999).
28. A. W. Sleight, H.-Y. Chen, and A. Ferretti, *Mater. Res. Bull.* **14,** 1571 (1979).